ACERP: Vol. 4, No. 3 & 4, (Summer & Fall 2018) 23-35

Advanced Ceramics Progress

Research Article

Journal Homepage: www.acerp.ir

An investigation on the effect of alumina on hydrothermal stability of nanostructured silica membrane prepared by sol-gel method

Maryam Shojaie-Bahaabad*, Reza Kaveh

Department of Chemical and Material Engineering, Shahrood University of Technology, Shahrood, Iran

PAPER INFO

Paper history:

Received 06 May 2019
Accepted in revised form 22 June 2019

Keywords:

Nanostructure silica
Silica-alumina membrane
Hydrothermal stability
Nanoporous membrane

ABSTRACT

In the present study, the effect of alumina on the pore structure and hydrothermal stability of nanostructured silica was investigated. SiO_2 and SiO_2-15wt%Al_2O_3 membranes were prepared by dip coating on mesoporous γ-Al_2O_3 coated macroporous α-alumina support. The particle sizes of sol were increased by adding of alumina to silica sol. Through the addition of the alumina up to 15 wt% and heat treatment at 500 °C, the silica structure was remained amorphous and the thickness of the top layer was in the range of 200-500 nm because of an increase in the sol viscosity. FT-IR analysis showed the formation of Si-O-Al bonds after heat treatment in the SiO_2-15wt%Al_2O_3 membrane. After placing the membranes under hydrothermal test, the pore volume and size were slowly decreased by means of alumina addition in that order. Furthermore, the permeability of gas molecules (H_2, He, CO_2,…) from the silica membrane was abruptly decreased compared to the SiO_2-15wt%Al_2O_3 membrane. Therefore, the membrane containing the added alumina had a more suitable hydrothermal stability due to the formation of more stable Si-O-Al bonds.

1. INTRODUCTION

The separation technology has been improved in industries to reduce their expenditures. Adsorption and separation using membrane are two developed technologies which represent a great advantage in research and improvement [1,2]. In the process of gases separation, four different membranes such as organic (polymeric), inorganic (ceramic), metallic and hybrid (polymeric-ceramic) materials have been utilized [3-6]. Ceramic membranes have several advantages, such as high mechanical strength, high longevity (10-14 years old), thermal and chemical stability, easy access, reasonable cost, high flux, selectivity and reliability [7]. These membranes have relatively narrow pore size distribution and are also suitable for high-pressure environments [7]. The selection material for membrane application is the first issue in designing of any separation process. Among ceramic membranes, silica-based ones are the most attractive because of their amorphous structure, pore sizes less than 1 nm, thickness control capability, access to high permeability flux, the feasibility of control the size and structure of the porosity and high selectivity [8]. The drawback of the silica membranes is its poor hydrothermal stability when they expose to the water and water vapor [9]. Therefore, improving the stability of these materials is an important issue to increase the separation efficiency of these membranes. Khatib [9] has investigated the thermal and hydrothermal stability of the silicon membrane prepared by the CVD method in the atmospheres of nitrogen gas at 440 °C and vapor pressure of 0.04 bar. The silica hydrothermal stability can be increased through hydrophobic silica with the addition of methyl groups in the silica network and heat treatment of the membrane under the water vapor [10], or providing a hybrid membrane of silica-organic material [11]. Moreover, the porous membranes with improved hydrothermal stability can be prepared using crystalline materials such as zeolites [12]. Because of the limitation in single crystal growth and the formation of a thin layer on the surface in zeolites, the resistance of these membranes against the gas permeation is higher than that of silica membranes.

* *Corresponding Author Email: mshojaieb@shahroodut.ac.ir (M. Shojaie-Bahaabad)*

Other methods for increasing the stability of the microporous silica network are the addition of metal [13-17] and metal oxides such as titanium, zirconium, iron, aluminium, chromium, cobalt, niobium, cerium and yttrium oxides [18-23]. Another approach is the development of ceramic membranes such as TiO_2, ZrO_2, and Al_2O_3 for the gas separation process in hydrothermal conditions [24]. These membranes are less efficient than the amorphous silica materials because it has less structural density than amorphous titanium, zirconium and aluminium [24]. Therefore, the amorphous silica has a more open structure with extra pores, which is more suitable for application in a gas separation unit [24]. Hence, the addition of a variety of additives to the silica is an effective method to improve the stability in steam. Kageyama [25] and Gu [26] have reported the hydrothermal stability of the silica-alumina membrane fabricated by the CVD method. In the present study, a defect-free and smooth silica-alumina nanoporous top layer was prepared by polymeric sol-gel method on an intermediate layer of gamma-alumina coated on the α-Al_2O_3 substrate. The effect of alumina on pore structure and hydrothermal stability of the nanostructured silica membrane was studied. To evaluate the membrane characteristics, DLS, FTIR, XRD, FESEM, N_2 adsorption-desorption methods and gas permeation test were used. It is intended to investigate the performance of silica-alumina membrane for the separation of binary gas mixtures like H_2/CO_2 or H_2/CH_4 in future researches.

2. MATERIALS METHOD

2.1. Alumina substrate preparation

Alumina substrates (2mm thickness and 1.7 cm diameter) were prepared by uniaxial pressing of α- Al_2O_3 powder (with a purity of 99.99 %, average particle size about 0.3 μm, French Baikalox) under the pressure of 150 psi. The substrates were sintered at 1400 °C for 2 h. Then, the surface of the substrate was polished with 400 to 1200 grit sandpapers, washed by deionized water and dried at 110 °C for 2 h.

2.2. PREPARATION OF ALUMINA COLLOIDAL SOL

The intermediate layer was coated using alumina colloidal sol to prepare the surface of the substrate for top layer deposition and reduction of the porosity gradient on the α-Al_2O_3 substrate. To prepare the colloidal sol, aluminium tri-sec-butylate ($C_{12}H_{27}AlO_3$, Merck), ethanol (Merck), polyvinyl alcohol (PVA, MW:72000, Merck), nitric acid 65% and distilled water were used as raw materials. At first, 5 mL aluminium tri-sec-butylate was added to the solvent, and the solution was stirred by a magnetic stirrer. After 30 min, water (molar ratio of water:aluminium alkoxide= 1:100) was added drop by drop to the solution to complete the hydrolysis reaction. After leaking the alcohol, nitric acid 1M was added to the solution as a flocculation agent. After the addition of the acid, the appearance of the solution was changed from milky to semi-transparent. At that time, the solution was refluxed for 16 h. Before coating, the polyvinyl alcohol solution was added to the alumina colloidal sol to control the drying stage of the intermediate layer.

2.3. Preparation of polymeric sol

The membrane top layers were prepared from the silica and silica-alumina polymeric sols. Because of the difference in the hydrolysis rate of aluminium and silicon alkoxides, each of the alumina and silica polymeric sol was first prepared separately and then added to each other. Initially, 50 mL of the silicon alkoxide (TEOS: Tetra-ethylorthosilicate, Merck, 99.99%) was dissolved in 30 mL of isopropanol alcohol, and after stirring for 30 min, 0.1 mL of the nitric acid was added to the solution. After stirring for 30 min, 2.5 mL of distilled water was added to the solution so that the transparent silica sol was obtained after stirring for 3 h. To prepare the alumina sol, aluminium isopropoxide (Merck, 99.99%) was added to isopropanol and the ransparent sol was obtained by adding the distilled water and stirring for 2 h. In the preparation of the silica-15wt% alumina sol, alumina sol was added to the silica sol drop by drop. SiO_2-15%Al_2O_3 polymeric sol was obtained after stirring for 2 h on a magnetic stirrer at a rate of 500 rpm.

2.4. Memberane preparation

At this stage, the alpha alumina substrate was coated by dipping method with the alumina colloidal sol and then polymeric silica and SiO_2-15%Al_2O_3 sols. The dip-coating process was performed using an automatic dip-coating device. The intermediate layer was deposited on top of the substrate with dipping and withdrawal speed of 10 mm/min and holding time of 10 s. The polymeric sols were coated on gamma-alumina layer with dipping and withdrawal speed of 5 and 30 mm/min, respectively and holding time of 50 s. The samples were maintained for 12 h in a container with a moisture content of 60% (measured by a moisture controller) and then were dried. The samples were heated at 80 °C with a heating rate of 0.5 °C/min and kept for 15 min at this temperature. Then, they were reached at the temperature of 110°C with the same heating rate and kept at the same temperature for 30 min. After heating at 200 °C and keeping the samples for 45 min, they were sintered at 500 °C for 1 h. It should be noted that to achieve the layers with appropriate quality and thickness, intermediate and top layers were prepared after coating and heating for 3 and 4 times, respectively [7]. Unsupported membranes were prepared by drying the sols onto a petri dish and heating at the desired temperature (500 °C) for 1 h.

2.5. Membrane characterization

A roughness test was implemented by roughness checker (Surtronic 25) to inspect the roughness of the substrate

surface. Apparent porosity of the substrate was measured based on the ASTM C20-92 standard. A dynamic lighter scattering analyzer (DLS, Malvern device ZEN3600) was used to measure the particle size distribution of the sols. Unsupported membranes were characterized by X-ray diffraction (XRD, Bruker AXS D-8 X-ray diffractometer with Kα waveform in length of 1/454.1 °A) and Fourier transform infrared (FTIR, Nexus Nicolet Spectrophotometer Nicolet IR100) at the range of 400-4000 cm^{-1} to determine the phases and bonds. Pore size distribution and specific surface area related to the unsupported membranes were measured by N_2 adsorption-desorption analysis (BET & BJH, Micrometric Tristar devices). Characterizations analyzes were carried out on the unsupported membranes by assuming that their properties are similar to those of the supported membranes. The topography and thickness of the membrane were observed by scanning electron microscope (SEM & FESEM, Hitachi 4160). Gas permeation tests were carried out in a house-developed set-up. Measurement of the single gas permeation was accomplished using bubble flow meter and gas chromatography (GC, 8430 magnetic) at 25 °C and pressure difference at both sides of the membrane was selected within the range of 1-8 bar. In order to tudy the hydrothermal stability, the membrane and unsupported membrane were first exposed to a water pressure of 0.56 bar at 110 °C for 72 h in an autoclave. The samples were then dried at 200 °C for 2 days.

3. RESULTS AND DISCUSSION

Alpha-alumina was selected as the support because of its high mechanical and chemical stability in the harsh environment [2]. The apparent porosity of the obtained substrate was 34%. According to the other reports, the proper apparent porosity for the support was 30-40% for the membrane preparation [1, 7, 23]. For coating of the perfect membrane layer on a macroporous substrate, it is necessary to modify the surface of the substrate to prevent film cracking (due to surface roughness) and infiltration of the solution into the substrates [23]. Therefore, the polishing of the substrate was proposed to meet these goals. The features of the substrates roughness are shown in Table 1. It is observed that the surface roughness has been reduced by comparing the polished and unpolished substrates.

Figure.1 shows the FESEM image of the surface and cross-section of the substrate after sintering. The support pore size should be large enough to build a pore size gradient from the support through the top layer. The gradient in the pore size effectively prevents early clogging of the membrane during its performance [2]. According to Figure.1, the substrate with pores having almost less than 300 nm size can be considered as the macroporous support.

TABLE.1. The roughness of unpolished and polished alumina substrate

	Average roughness (µm)	Maximum height of peak (µm)	Maximum depth of valley (µm)
Unpolished substrate	1.67	2.86	6.97
Polished substrate	0.394	1.78	1.84

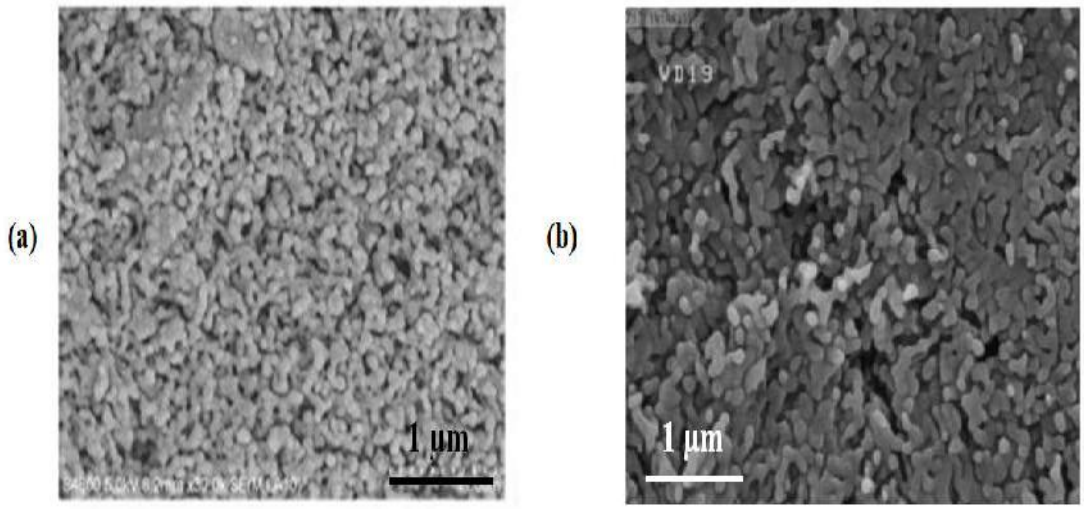

Figure 1. FESEM image of a) cross section and b) surface of alpha-alumina substrate

When the substrate exposes to the polymeric sol, the infiltration of the sol particles leads to partial obstruction of the substrate porosity in later stages that results in a resistance against the gas permeation which is undesirable. Branches should be formed at the entrance of the pores, to prevent the excessive infiltration of the polymeric sol particles into the pores of the substrate.This stage is called the first step of the film formation. Using dipping sol containing larger particles before polymeric SiO_2-15%Al_2O_3 sol inhibits the infiltration of the particles into the substrate pores. Consequently, it is required to use the alumina colloidal sol to coat the intermediate layer. Figure.2 displays the particle size distribution of both sols without and with PVA additive. As can be seen, the maximum particle size in the alumina sol without and with PVA was 37 nm and 40nm correspondingly. According to the particle size distribution curve, the particle sizes of the alumina colloidal sol are in the range of 20 to 90 nm. PVA addition is led to increasing the viscosity and agglomeration of the particles and a slight shift in the particle size distribution chart toward the larger particle size. To investigate the stability of the colloidal, zeta potential was measured. Zeta potential of the prepared colloidal sol was 44 mV. According to the literature, stable alumina colloidal sols have zeta potential higher than 41 mV [27].

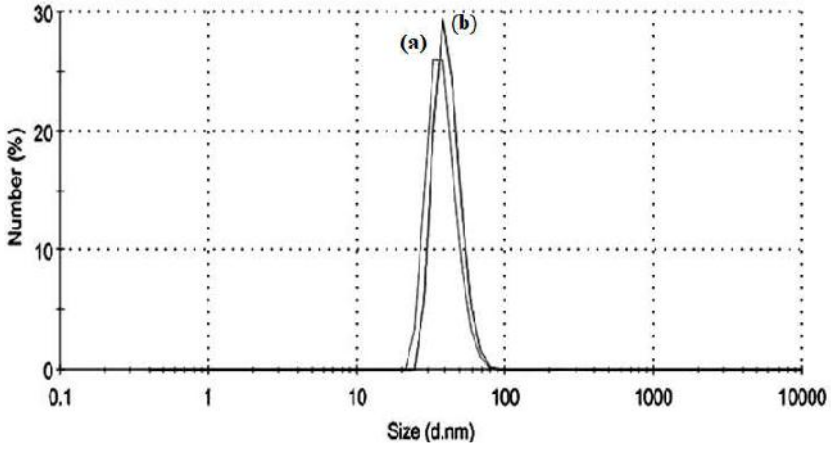

Figure 2. The particle size distribution of boehmite colloidal sol a) without PVA and b) with PVA obtained by DLS

The intermediate layer must be as the mesoporous structure and has enough mechanical and chemical stability. The γ-Al_2O_3 intermediate layer is appropriate to achieve these properties simultaneously. X-ray diffraction pattern of prepared the colloid sol in order to cover the intermediate layer after calcination at 600 °C for 3 h is presented in Figure.3. As can be seen that the γ-Al_2O_3 peaks are observable. Similar results have been reported in another research work [23].

N_2 adsorption-desorption isotherm and BJH pore size distribution of the unsupported γ-Al_2O_3 intermediate layer after calcination at 600°C are shown in Figure. 4. In accordance with the IUPAC standard, the adsorption isotherm shows a type IV one with an H2 hysteresis loop which is a representative of the mesoporous substances with the pores in the form of bottle ink (see Figure.4a) [1]. According to Fig. 4b, the pore diameters varies in the range of 2 to 100 nm and the average pore size, which is calculated by the BJH method, is about 8 nm. This result indicates that a major fraction of the pores is in the mesopore range.

The FESEM image of the intermediate layer surface on the α-Al_2O_3 substrate before and after polishing is shown in Figure. 5a. When surface roughness increases, the sol particles trap in the cavities of the rough surface and cause non-uniformity and non-continuity in the intermediate layer which is coated on the substrate. As can be seen in Figure.5b, after polishing, the layer surface was continuously and without imperfections formed. Figures 5c and 5d present the effect of the PVA on the formation of the γ-Al_2O_3 intermediate layer. In fact, because of the penetration of small particles to the substrate, the intermediate layer does not form before the addition of the PVA. The particles stay together due to the interparticle connection after the PVA addition. As a result, the intermediate layer is deposited with a thickness less than about 460 nm (see Figure. 5d). The particle size distribution of the polymeric silica and SiO_2-15Al_2O_3 sols are shown in Figure. 6. According to the curves, a significant fraction of the particles of the polymeric sols has a diameter less than 1nm, and their particle size is in the range of 0.5-5 nm.

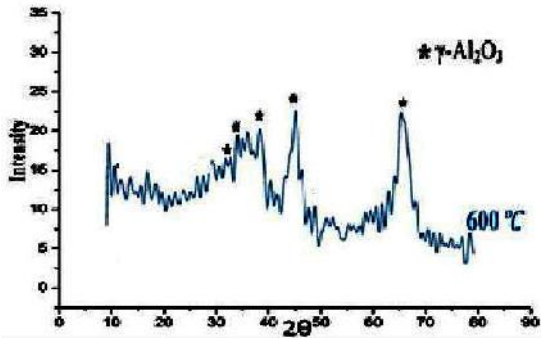

Figure 3. XRD pattern of boehmite xerogel calcined at 600 °C for 3 h

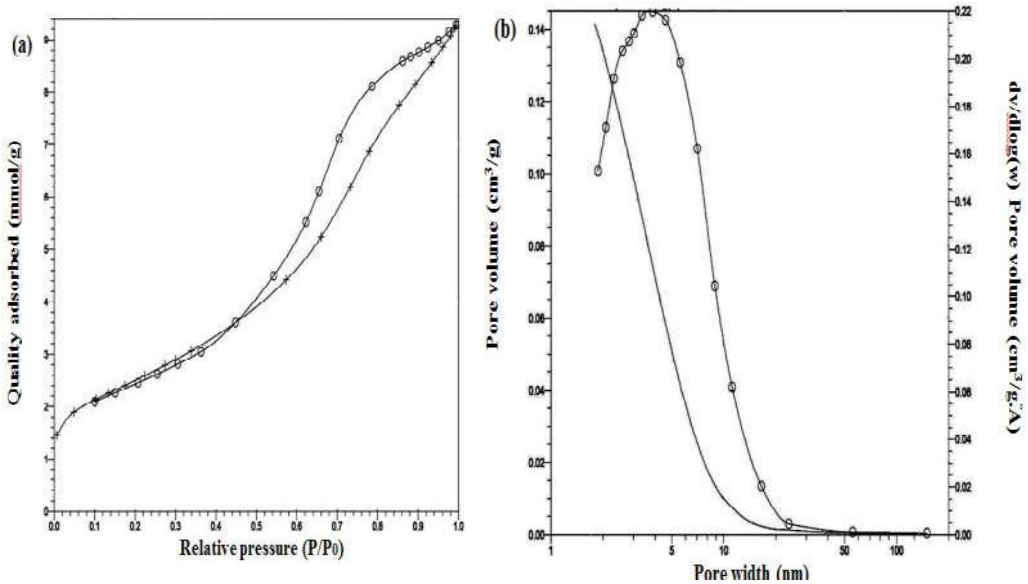

Figure 4. a) N_2 adsorption-desorption isotherm and b) pore size distribution of gamma-alumina unsupported membrane calcined at 600 °C for 3 h

It seems that using low water levels in the preparation of the polymeric sols is led to reduce the hydrolysis rate of the aluminum alkoxides which is caused forming particles with nanometric dimensions in the sols [23]. According to the obtained graphs, the average particle size in the sol is increased with the addition of alumina, and the particle size distribution becomes wider. According to the studies, the silicon alkoxides ($Si(OR)_4$) have no significant activity for the water reaction. However, aluminum alkoxide has a higher reaction rate with the water and is hydrolyzed as soon as contact with the water during an exothermic hydrolysis reaction. For that reason, the aluminum alkoxide rapidly consumes the water in the sol so that the concentration of the sol increases. As a final point, the probability of the agglomeration and growth of the particles increases.

Infrared Fourier-transform spectroscopy (FTIR) is a proper and developed method for determining chemical bonding of the mixed oxides. The results of this analysis are shown in Fig. 7. In the FTIR spectroscopy pattern, the absorption band at 470.53 cm^{-1} shows the presence of Si-O-Al bonding [28]. The symmetric and asymmetric stretching vibrations of Si-O-Si also show the bands at 1054 cm^{-1} and 1094.49 cm^{-1}, respectively [28]. The peak at 799.83 cm^{-1} is attributed to the Al-OH band [28]. Moreover, the peaks at 1630, 3198, 3740, and 3400 cm^{-1} indicate the presence of the hydroxyl groups and water which is absorbed by the sample in the environment [29].

The possible mechanism in this system can be divided into two steps. In the first one, TEOS alkoxide is hydrolyzed, and Si-OH groups are formed. These groups form Si-O-Si chains during the condensation process. It should be noted that the polymeric molecules ($Si(OH)_4$) absorb aluminum ions because of the reaction between silicon and aluminum. These ions break the Si-O-Si bands and form the Si-O-Al linkages [28, 29].

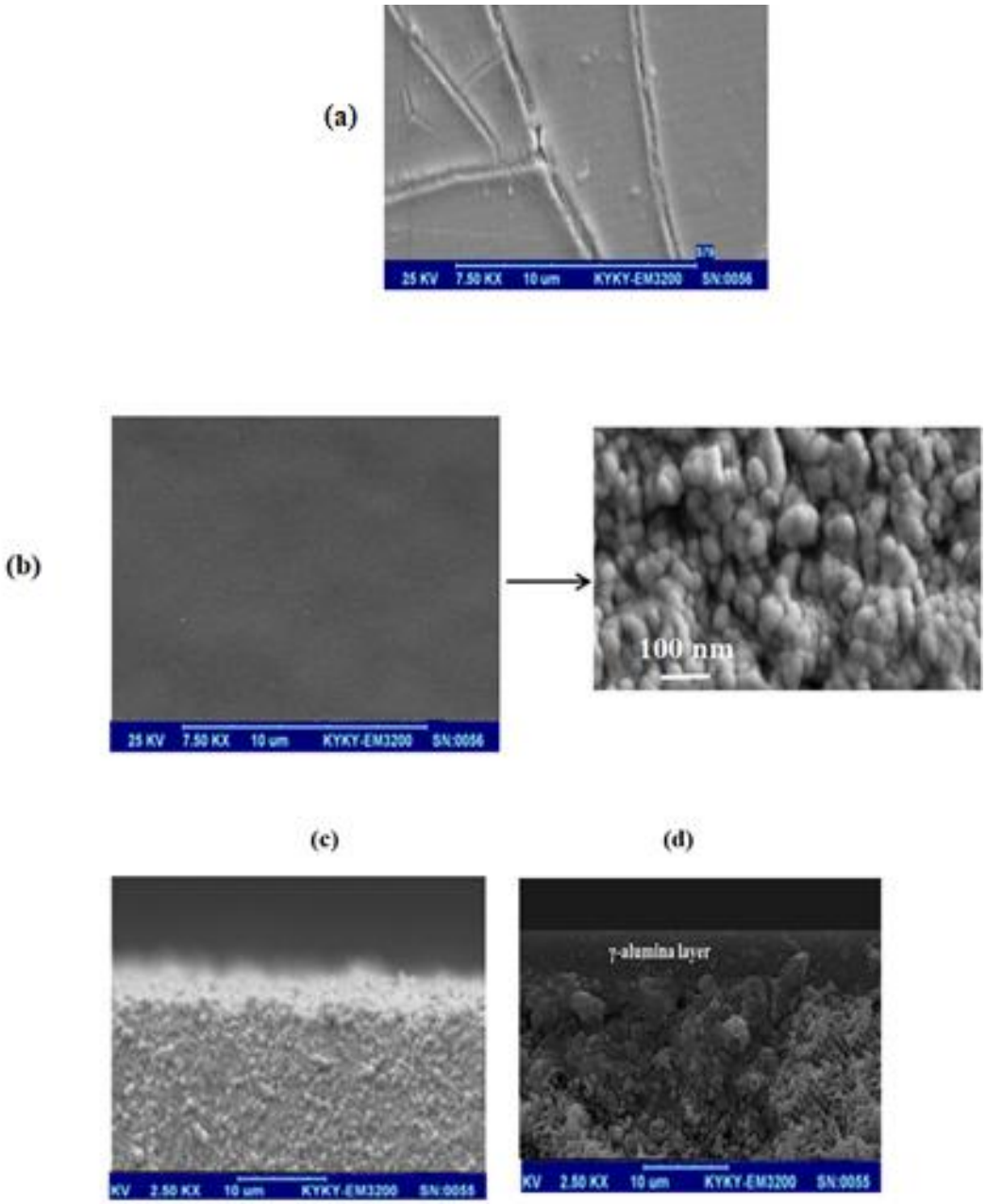

Figure 5. a) The surface of the gamma-alumina intermediate layer deposited on a) unpolished substrate, b) polished substrate and cross-section of the gamma-alumina intermediate layer deposited on polished substrate c) without PVA addition, d) with PVA addition calcined at 600°C for 3h

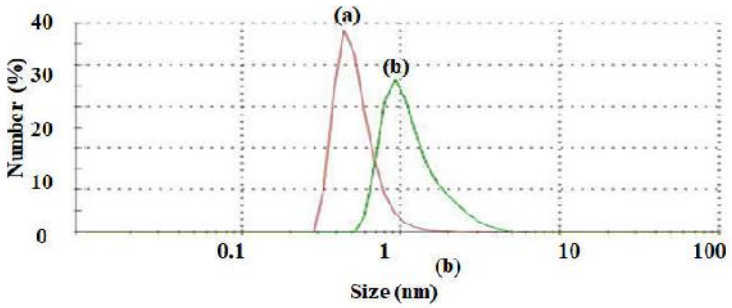

Figure 6. The particle size distribution of a) silica and b) silica-15% alumina polymeric sols obtained by DLS

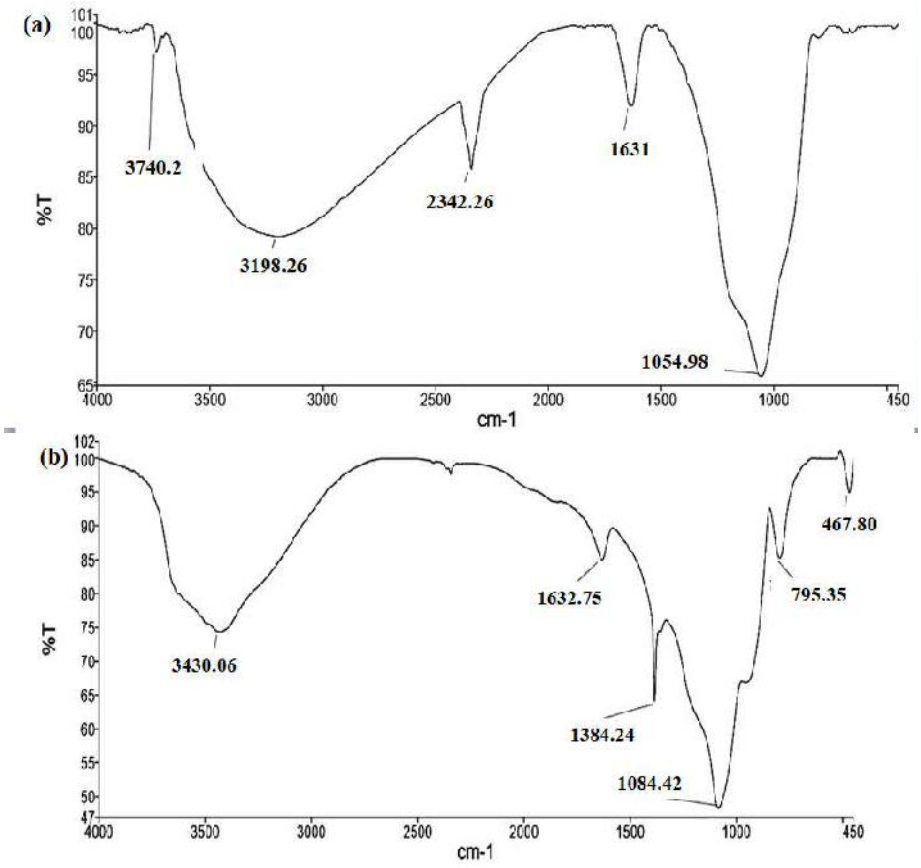

Figure 7. FT-IR spectra of a) silica and b) silica-15%alumina unsupported membranes heat-treated at 500 °C for 1 h

As can be seen, in the diffraction pattern of Figure. 8, SiO_2-15%Al_2O_3 gel is amorphous at 500 °C, and there is no crystalline phase in it which indicates the lack of separation of two phases of silica and alumina. Therefore, the presence of the alumina in the silica network does not cause the crystallization of the silica.

As seen from FESEM images (Figure. 9), a defect-free layer with a thickness of between 200 to 500nm is formed on the γ-Al_2O_3 intermediate layer. The obtained layer thickness is increased by adding the alumina in the sol because the sol viscosity increases from 2.38 to 10.25cP. Thus, the infiltration amount of the sol into the substrate decreases and the thickness of the layer increases.

To investigate the effect of the alumina on the hydrothermal stability of the silica, N_2 adsorption-desorption analysis was performed on the silica and SiO_2-15%Al_2O_3 unsupported membranes. According to the BET isotherms (Figure. 10a and 10b) and comparison of these isotherms with the adsorption ones, which are provided by IUPAC, it can be seen that these isotherms are corresponded to the I-type adsorption isotherm, suggesting the microporous structure of the membranes slit-like pores [30]. The absence of the hysteresis loop and coincidence of the adsorption isotherm with desorption one are initiated from the presence of the micropores with dimensions less than 2 nm [31, 32]. The factors that can cause the closing of the hysteresis loop are increased the interconnecting of the pores or reduced the meandering of them [31]. Accordingly, it can be claimed that the synthesized membranes have very small and uniform pores which are desirable for the permeation of small gas molecules. The surface area and volume of pores, which were obtained established upon the BJH analysis, are about 344.32 m^2/g, 0.23 cm^3/g, and 303.05 m^2/g, 0.17 cm^3/g for unsupported silica membrane and unsupported silica-15% alumina membrane, respectively. Figures 10c and 10b show the pore distribution obtained by the BJH. In this study, the reported mean pore diameter was 1.96 nm and 2.04 nm for silica and silica-15%alumina membrane, correspondingly. It is worthy to note that the pore size lower than 1.8 nm is not detectable. It has been reported that the BJH curve typically has one or two peaks [23]. As a result, the pore diameters are increased by adding the alumina. Anyway, some pores are smaller than 1.8nm. Therefore, the silica-15%alumina can be considered as a gas separation membrane. The pore size in the sol-gel method depends on the size of the primary particle size in the sol. According to the DLS analysis, the particle sizes of the sol are increased through the addition of the alumina, and then the pore size is also increased.

Figures 11a and 11b indicate that the pore sizes of the unsupported membranes increases after hydrothermal test, as for the microporous materials, the I-type of the adsorption isotherm changes to the IV-type. Therefore, the pore sizes are increased due to the presence of the moisture. According to the adsorption-desorption isotherms, it can be said that the silica-15%alumina membrane with the closer hysteresis loop has a higher uniformity in pores. In relation to Figure. 11c, after hydrothermal test, the pore size distribution of the unsupported silica membrane was in the range of 1.96 to 40 nm with an average pore diameter around 2.6 nm as calculated by the BJH method.

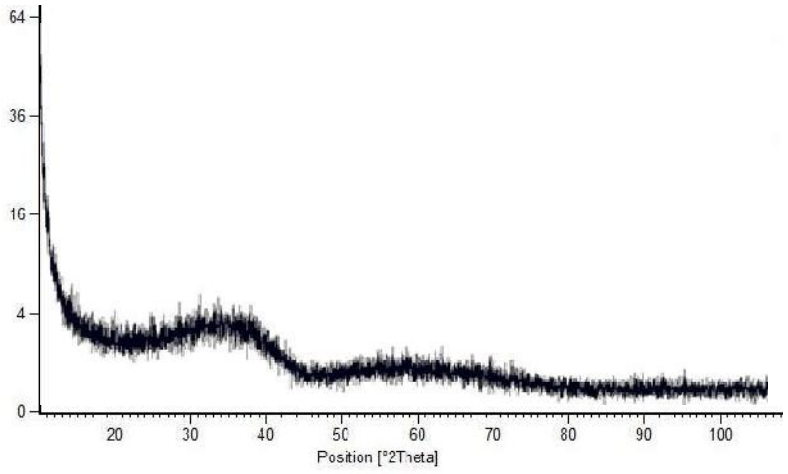

Figure 8. XRD pattern of silica-15%alumina membrane heat-treated at 500 °C for 1 h

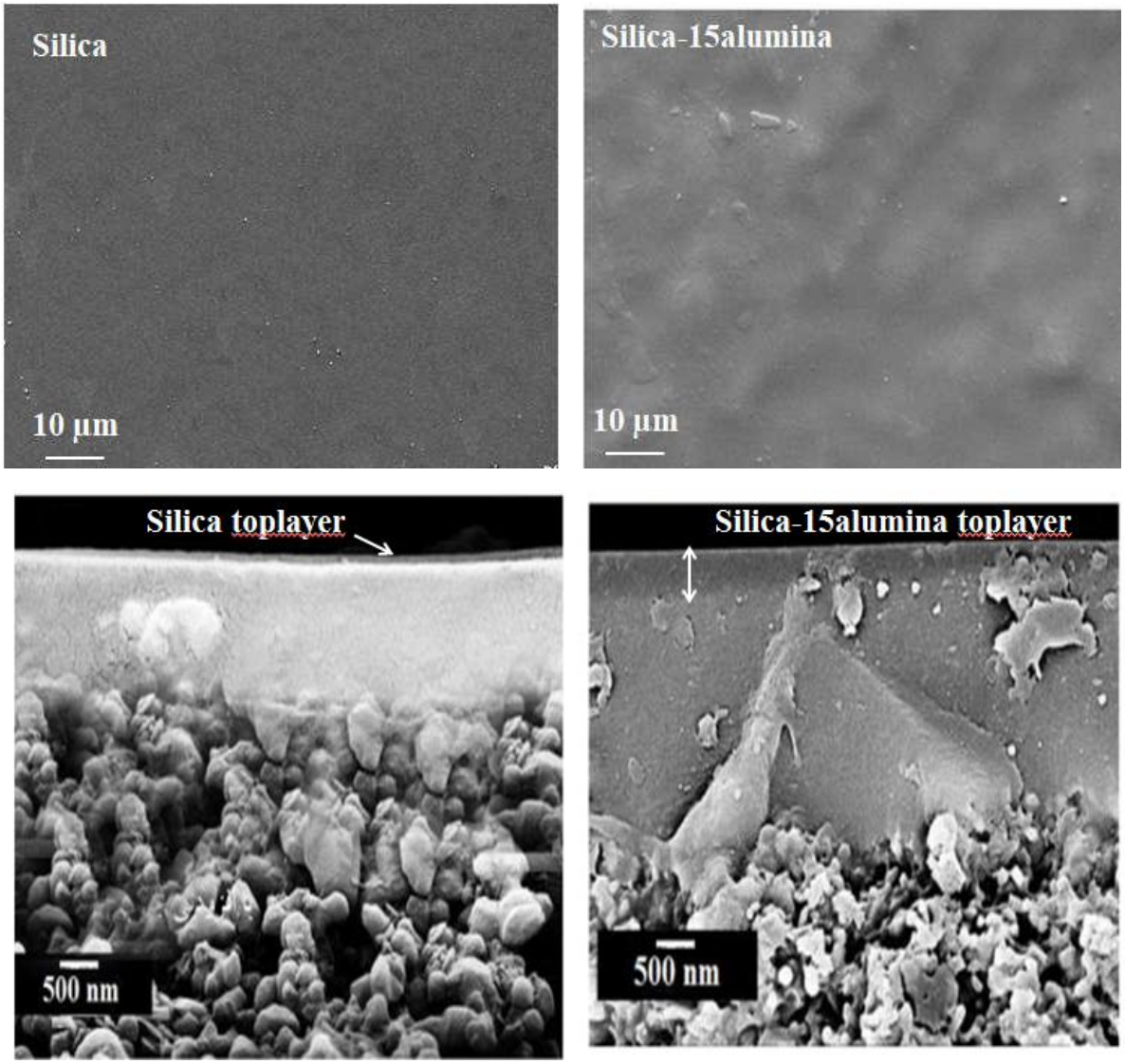

Figure 9. Surface and cross-sectional images of silica and silica-15%alumina membranes heat-treated at 500 °C for 1 h

For the silica-15% alumina unsupported membrane, the pore size distribution was in the range of 1.96 to 20 nm with an average pore diameter around 2.7 nm. Based on these results, after hydrothermal test, the surface area and pores volume decrease to 223.42 m^2/g and 0.11 cm^3/g, respectively, obtained from the amount of N_2 adsorbed at P/P_0 of 0.97. Furthermore, these values decrease to 297.38 m^2/g and 0.13 cm^3/g in that order for the silica-15%alumina unsupported membrane. According to BJH results, pore sizes increase in all specimens after exposing to hydrothermal conditions for 72 h. Nevertheless, as can be seen, the drop rate in structural parameters in SiO2-15%Al2O3 unsupported membrane is lower because of their more stability and compact structure. The results of the single gas permeability test for the silica and SiO2-15%Al2O3 membranes before and after the hydrothermal test are shown in Table 2. These results allow estimation of the pore size distribution of the membranes. Assuming that the resulting membranes act as a size-based sieve, the low permeation for a specific gas corresponds to a small number of pores that are accessible for those species.

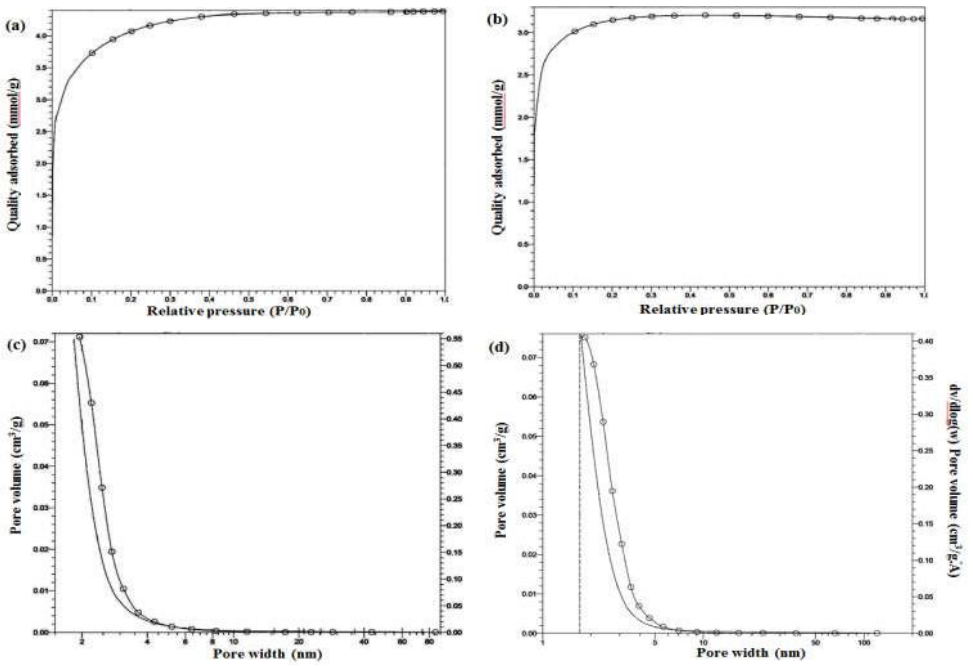

Figure 10. a) N_2 adsorption-desorption isotherm and pore size distribution of a,c) silica unsupported membrane and b,d) silica-15%alumina unsupported membrane calcined at 500 °C for 1 h before the hydrothermal test

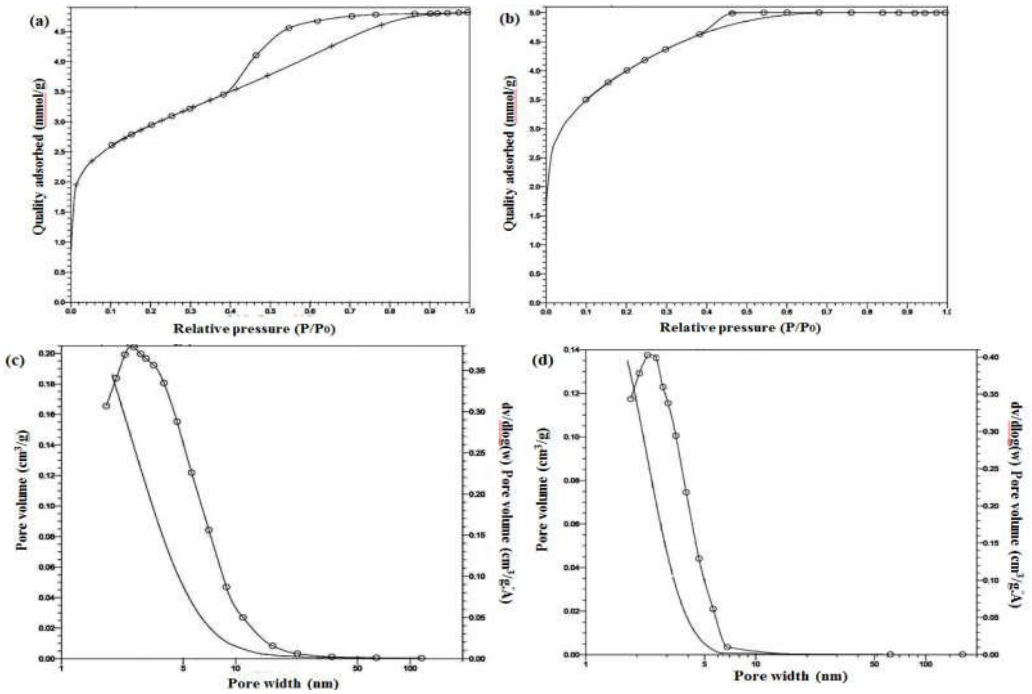

Figure 11. a) N_2 adsorption-desorption isotherm and pore size distribution of a,c) silica unsupported membrane and b,d) silica-15%alumina unsupported membrane calcined at 500 °C for 1 h after the hydrothermal test1

In general, it was observed that the permeation of the gas molecules is decreased by increasing kinetic diameter. The SF6 permeance of the pure silica membrane is so low, as it is not easily measurable. Concerning these results, it can be expressed that most pores in the pure silica membrane are between 0.3-0.4 nm, and very few of them have a diameter greater than 0.55 nm. The helium permeance of the SiO_2-15%Al_2O_3 membrane was almost fifteen times larger than N_2 and CH_4. This means that a large fraction of pores is smaller than the size of nitrogen and methane. In comparison to the pure silica membrane, the flow rate of SF6 gas is higher. It suggests that the fraction of pores is larger than 0.55 nm. Various gases permeances decrease from SiO_2-15%Al_2O_3 membrane whereas the larger molecules permeances do not change after the hydrothermal test. This issue recommends that there are not any cracks on the surface after the hydrothermal test.

TABLE 2. Single gas permeance of silica and silica-15%alumina membranes before and after the hydrothermal test

Gas molecule	Kinetic diameter (nm)	Permeance of SiO_2 membrane * 10^{-6} (mol/m².Pa.s)		Permeance of SiO_2-15%Al_2O_3 membrane * 10^{-6} (mol/m².Pa.s)	
		Before hydrothermal test	After hydrothermal test	Before hydrothermal test	After hydrothermal test
He	0.26	8.5	4.8	1	0.82
H_2	0.29	6.5	2.2	0.9	0.61
CO_2	0.33	0.63	0.2	0.58	0.58
O_2	0.35	0.59	0.15	0.55	0.5
N_2	0.36	0.55	0.14	0.47	0.47
CH_4	0.38	0.43	0.005	0.41	0.40
SF_6	0.55	0.0095	0.0001	0.0095	0.0095

According to Table 2, the permeability in the pure silica membrane is much higher than the SiO_2-15Al_2O_3 one. It seems that by adding aluminum ions to the silica network, a material is obtained which has more condensed structure than the pure silica. Oxygen forms more stable and polar bonds with aluminum than with silicon. Furthermore, aluminum has a coordination number higher than the silicon, thus, it tends to form a more condensed structure than the pure silica. Consequently, it expects that the silica membrane reinforced with aluminum has more closely packed and stable structure than the pure silica. For this reason, the gas molecules permeance of the SiO_2-15%Al_2O_3 membrane decreases. Besides, after the hydrothermal test, it was observed that the gas permeance of the alumina-containing membrane is reduced at a lower rate. The unsustainability of amorphous silica mainly relates to its hydrophile nature. Si-O-Si linkages were broken when they subject to the steam reaction and formed Si-OH hydroxyl pairs. It exposes to a recondensation process at a higher temperature. This structural perturbation and rearrangement of Si-O-Si bonds make the structure more flexible. In this state, it is possible that the network is organized into a very stable state and formed a dense network. The condensation process of a microporous material in the hydrothermal condition is similar to the sintering process. Indeed, when the sintering progresses, the mesoporous material tends to reduce the pore volume and increases the pore size in a hydrothermal environment. It expects that this phenomenon is more severe in the case of microporous silica. In the microporous silica, pores have higher curvature than the other mesoporous materials so that they are filled already by water even at relatively low vapor pressure. In the case of microporous materials used for the gas separation process, the structural perturbation and rearrangement process can lead to creating a complete dense material. Therefore, after the membranes were placed under the hydrothermal test, gas molecules permeance of the membranes decreases. Considering the results, the hydrothermal stability was improved by adding the alumina so that the decrease in the gas molecules permeance occurs at the lower rate. The higher stability of the SiO_2-15%Al_2O_3 can be due to the following reasons:

1. Microporous amorphous structures are not stable thermodynamically and tend to be condensed [18]. One of the reasons for the higher stability of the SiO_2-15%Al_2O_3 membrane was the presence of larger pores compared to the silica one. Pores with higher curvature (small pores) are more sensitive to the hydrothermal environment than large pores having smaller curvature.
2. After the addition of the alumina, Si-O-Si bonds are replaced by Si-O-Al ones. Aluminum ions create more polar and stable bonds with silica. Therefore, Si-O-Al linkages are not easily broken when the SiO_2-15%Al_2O_3 membrane subjects to the steam. In this way, the

hydrothermal stability of the silica membrane is improved.
3. Due to the high coordination number of these ions, the structure of the SiO_2-15%Al_2O_3 membrane is denser and therefore has more stability.

4. CONCLUSION

Silica membrane and silica-15wt%alumina membranes were prepared, and then its properties were investigated before and after coating on the alumina substrate. The size of the sol particles was increased with the addition of alumina to the silica sol. According to the FT-IR analysis, the formation of the Si-O-Al bonds was proved. It was found that by adding alumina to the silica membrane up to 15 wt% and subsequently heat treating at 500 °C, the crystalline phase was not observed in an X-ray diffraction pattern. According to the BJH analysis, the pore sizes were increased with the addition of alumina. The membrane thickness was also increased with the addition of alumina to the silica membrane because of an upsurge in viscosity of the sol. Adding alumina was caused to increase the hydrothermal stability of the silica membrane so that the permeability of the gas molecules was decreased with a lower rate.

REFERENCES

1. Tajer-Kajinebaf, V., Sarpoolaky H., Mohammadi, T., "Synthesis of Nanostructured Anatase Mesoporous Membranes with Photocatalytic and Separation Capabilities for Water Ultrafiltration Process", ***Iranian Journal of Materials Science and Engineering***, Vol. 10, (2013), 37-45.
2. Tajer-Kajinebaf, V., Sarpoolaky, H., Mohammadi, T., "Sol–gel Synthesis of Nanostructured Titania–Silica Mesoporous Membranes with Photo-degradation and Physical Separation Capacities for Water Purification", ***Ceramics International***, Vol. 4, (2014), 1747-1757.
3. El Hawa, H.W.A., Paglieri, S.N., Morris, C.C., Harale, A., Way, J.D., "Application of a Pd-Ru Composite Membrane to Hydrogen Production in a High Temperature Membrane Reactor", ***Separation and Purification Technology***, Vol. 147, (2015), 388-397.
4. Shafiee, A., Arab, M., Lai, Z., Liu, Z., Abbas, A., "Modelling and Sequential Simulation of Multi-Tubular Metallic Membrane and Techno-Economics of a Hydrogen Production Process Employing Thin-Layer Membrane Reactor", ***International Journl of Hydrogen Energy***, Vol. 41, (2016), 19081-19097.
5. Zhang, X.L., Yamada, H., Saito, T., Kai, T., Murakami, K., Nakashima, M., Ohshita, J., Akamatsu, K., Nakao, S.I., "Development of Hydrogen-Selective Triphenylmethoxysilane-Derived Silica Membranes with Tailored Pore Size by Chemical Vapor Deposition", ***Journal of Membrane Science***, Vol. 499, (2016), 28-35.
6. Matsuyama, E., Ikeda, A., Komatsuzaki, M., Sasaki, M., Nomura, M., "High-Temperature Propylene/Propane Separation through Silica Hybrid Membranes", ***Separation and Purification Technology***, Vol. 128, (2014), 25-30.
7. Biglu, Y.F.G., Taheri-Nassaj, E., "Synthesis and Characterization of Alumina Supported Sub-nanoporous SiO_2–10 wt%TiO_2 Membrane for Nitrogen Separation", ***Journal of Industrial and Engineering Chemistry***, Vol.19, (2013), 1752-1759.
8. Kanezashi, M., Sasaki, T., Tawarayama, H., Tsuru, T., "Hydrogen Permeation Properties and Hydrothermal Stability of Sol–Gel-Derived Amorphous Silica Membranes Fabricated at High Temperatures", ***Journal of American Ceramic Society***, Vol. 96, (2013), 1-8.
9. Khatib, S.J., Oyama, S.T., "Silica Membranes for Hydrogen Separation Prepared by Chemical Vapor Deposition (CVD)", ***Separation and Purification Technology***, Vol. 111, (2013), 20-42.
10. Mingjuan, S., Chenglong, Z., Guoxing, N., Dongyuan, Z., "Improving the Hydrothermal Stability of Mesoporous Silica SBA-15 by Pre-treatment with $(NH_4)_2SiF_6$", ***Chiness Journal of Catalysis***, Vol. 33, (2012), 140–151.
11. Oyama, S.T., "Review on mechanisms of gas permeation through inorganic membranes", ***Journal of the Japan Petroleum Institute***, Vol. 54, (2011), 298-309.
12. Peng, L.C., "Biomodal Porous Ceramic Membrane via Nanosized Polysterene Templating: Synthesis, Characterization and Performance Evaluation", Proceedings of the Volume Doctor of Philosophy, USM., (2008).
13. Uhlmann, D., Smart, S., "High Temperature Steam Investigation of Cobalt Oxide Silica Membranes for Gas Separation", ***Separation and Purification Technology***, Vol. 26, (2010), 222–228.
14. Yang, J., Chen, J., "Silver-Doped Organic-Inorganic Hybrid Silica Membranes by Sol–gel Method: Preparation and Hydrothermal Stability", ***Separation Science and Technology***, Vol. 46, (2011), 2228–2232.
15. Tsurud, T., "Development of Metal-doped Silica Membranes for Increased Hydrothermal Stability and Their Applications to Membrane Reactors for Steam Reforming of Methane", ***Journal of the Japan Petroleum Institute***, Vol. 54, (2011), 277-286.
16. Qi, H., Chen, H., Li, L., Zhu, G., Xu, N., "Effect of Nb Content on Hydrothermal Stability of a Novel Ethylene-bridged Silsesquioxane Molecular Sieving Membrane for H_2/CO_2 Separation", ***Journal of Membrane Science***, Vol. 421, (2012), 190-200.
17. Liu, E., Wang, M., Hu, H., Liang, Y., Wang, Y., Cao, W., Wang, X., "High-Temperature Synthesis of Highly Hydrothermal Stable Mesoporous Silica and Fe–SiO_2 Using Ionic Liquid as a Template", ***Journal of Solid State Chemistry***, Vol. 184, (2011), 509-515.
18. Boffa, V., Blank, D. H., Elshof, J.E., "Hydrothermal Stability of Microporous Silica and Niobia-Silica Membranes, ***Journal of Membrane Science***, Vol. 319, (2008), 256-263.
19. Ahn, S.J., Takagaki, A., Sugawara, T., Kikuchi, R., Oyama, S.T., "Permeation Properties of Silica-Zirconia Composite Membranes Supported on Porous Alumina Substrates, ***Journal of Membrane Science***, Vol. 526, (2017), 409-416.
20. Puthai, W., Kanezashi, M., Nagasawa, H., Tsuru, T., "Nanofiltration Performance of SiO_2-ZrO_2 Membranes in Aqueous Solutions at High Temperatures", ***Separation and Purification Technology***, Vol. 168, (2016), 238-247.
21. Puthai, W., Kanezashi, M., Nagasawa, H., "SiO_2-ZrO_2 Nanofiltration Membranes of Di□erent Si/Zr Molar Ratios: Stability in Hot Water and Acid/alkaline Solutions", ***Journal of Membrane Science***, Vol. 524, (2017), 700-711.
22. Puthai, W., Kanezashi, M., "Development and Permeation Properties of SiO_2-ZrO_2 Nanofiltration Membranes with a MWCO of<200", ***Journal of Membrane Science***, Vol. 535, (2017), 331-341.
23. Khanmohammadi, S., Taheri-Nassaj, E., "Micro-porous Silica–Yttria Membrane by Sol–gel Method: Preparation and Characterizatio", ***Ceramics International***, Vol. 40, (2014), 9403-9411.
24. Van Gestel, T., Sebold, D., Hauler, F., Meulenberg, W.A., Buchkremer, H.P., "Potentialities of Microporous Membranes for H_2/CO_2 Separation in Future Fossil Fuel Power Plants: Evaluation of SiO_2, ZrO_2, Y_2O_3– ZrO_2 and TiO_2–ZrO_2 Sol–Gel Membranes", ***Journal of Membrane Science***, Vol. 354, (2010), 64-24.

25. Kageyama, N., Takagaki, A., Sugawara, T., Kikuchi, R., Oyama, S.T., "Synthesis and Characterization of a Silica-Alumina Composite Membrane and Its Application in a Membrane Reactor", ***Separation and Purification Technology***, Vol. 195, (2018), 437-445.
26. Gu, Y., Hacarlioglu, P., Oyama, S.T., "Hydrothermally Stable Silica–Alumina Composite Membranes for Hydrogen Separation", ***Journal of Membrane Science***, Vol. 310, (2008), 28-37.
27. Xina, W., Xiujian, Z., Chengbin, J., Haizheng, T., Jianjun, H., "Effects of Nitric Acid Concentration on the Stability of Alumina Sols", ***Journal of Wahan University of Technology-Materials Science Education***, Vol. 21, (2006), 102.
28. Roy, J., Bandyopadhyay, N., Das, S., Maitra, S., "Studies on the Formation of Mullite from Diphasic alumina-silica Gel by Fourier Transform Infrared Spectroscopy", ***Iranian Journal Chemical Engineering***, Vol. 30, (2011), 225-238.
29. Roy, J., Maitra, S., "Synthesis and Characterization of Sol-Gel-Derived Chemical Mullite", ***Journal of Ceramic Science and Technology***, Vol. 5, (2014), 52-62.
30. Sing, K., "Reporting Physisorption Data for Gas/Solid Systems with Special Reference to the Determination of Surface Area and Porosity", ***Pure Applied Chemistry***, Vol. 57, (1985), 603-624.
31. Oyama, S.T., Lee, D., Hacarlioglu, P., Saraf, R.F., "Theory of Hydrogen Permeability in Nonporous Silica Membranes", ***Journal of Membrane Science***, Vol. 244, (2004), 45–53.
32. Patterson, V.A., Krieg, H.M., Kriek, R.J., Bisset, H., "Direct Synthesis of a Titania Membrane on a Centrifugally Casted Tubular Ceramic Support", ***Journal of Membrane Science***, Vol. 285, (2006), 2006.